The dual role of Cr^{3+} in trapping holes and electrons in lanthanide co-doped GdAlO$_3$ and LaAlO$_3$

Luo, Hongde; Dorenbos, Pieter

Important note
To cite this publication, please use the final published version (if applicable).
Please check the document version above.

Journal of
Materials Chemistry C

Accepted Manuscript

Volume 4 | Number 1 | 7 January 2016 | Pages 1–224

Journal of
Materials Chemistry C

Materials for optical, magnetic and electronic devices
www.rsc.org/MaterialsC

ISSN 2050-7526

ROYAL SOCIETY
OF CHEMISTRY

PAPER
Nguyễn T. K. Thanh, Xiaodi Su et al.
Fine-tuning of gold nanorod dimensions and plasmonic properties using the Hofmeister effects

175 YEARS

ROYAL SOCIETY
OF CHEMISTRY

rsc.li/materials-c

The dual role of Cr^{3+} in trapping holes and electrons in lanthanide co-doped GdAlO$_3$ and LaAlO$_3$

Hongde Luo and Pieter Dorenbos

Delft University of Technology,

Faculty of Applied Sciences,

Department of Radiation Science and Technology,

Section Luminescence Materials,

Mekelweg 15, 2629 JB Delft, Netherlands

email:p.dorenbos@tudelft.nl

tel: +31 15 2781336

(Dated: April 16, 2018)

Abstract

Trivalent Nd, Dy, Ho, Er, Tm, Sm, Eu usually act as electron trapping centers in wide band gap compounds, whereas trivalent Ce, Tb, and Pr act as hole trapping centers. When a deep electron trap is combined with a shallow hole trap, then during the thermoluminescence glow the hole is released generating recombination luminescence at the electron trap. However in case of a shallow electron trap, the electron will be released to recombine at the hole trapping center. With the knowledge on location of the lanthanide levels within the band gap one may engineer the depth of the electron trap, the depth of the hole trap, and where the recombination will take place. This all has been tested and verified for the lanthanides in GdAlO$_3$ in [Luo *et al.* J. Phys. Chem. C 120 (2016) 5916.]. In this work Cr^{3+} is combined with various trivalent lanthanides in GdAlO$_3$. By combining thermoluminescence with optical spectroscopy data, a consistent interpretation of all data is obtained. Cr^{3+} can, other than all lanthanides, act both as a deep electron trap and as deep hole trap. From the results we will deduce the location of the Cr^{2+} and Cr^{3+} levels within the band gap and with respect to the vacuum level. Besides thermoluminescence recombination via the conduction band, evidence is found for athermal (tunneling) recombination. Results on GdAO$_3$ are compared with results on LaAlO$_3$. A related system but with lower lying conduction band and higher lying valence band that reduces the trap depths of the lanthanides and Cr in a predictive fashion.

I. INTRODUCTION

Methods and techniques to determine the location of the divalent and trivalent lanthanide levels within the band gap of compounds are now well-established. One may construct so-called vacuum referred binding energy (VRBE) schemes that then predict luminescence and carrier trapping properties [1]. Knowledge on what lanthanide will trap a hole and what lanthanide will trap an electron together with the trapping depths provides an engineering tool. One may combine a shallow electron trap with a deep hole trap, and then during TL the electron is released to yield the luminescence at the hole trapping lanthanide. Ce^{3+} often acts as a deep hole trap. One may also combine a shallow hole trap like Pr^{3+} with a deep electron trap like Eu^{3+}. Hole release from Pr^{4+} then yields the red recombination luminescence of Eu^{3+}. Past years studies have appeared on phosphates, germanates, aluminates, oxynitrides, nitrides that demonstrate those engineering concepts [2–8].

For applications, Cr^{3+} as a trapping and recombination center has received interest in persistent luminescence studies. Its emission in the infrared can be utilized for in vivo bio-imaging [9–13]. When we have information on where to expect the Cr^{2+} and Cr^{3+} levels within the band gap one may combine Cr^{3+} with a lanthanide ion and again engineer carrier storage and luminescence properties. A first study into that direction was reported by Ueda *et al.* [14, 15] on the $Y_3(Al_{1-x}Ga_x)_5O_{12}:Ce^{3+},Cr^{3+}$ garnet systems. Katayama *et al.* [16, 17] studied lanthanides combined with Cr^{3+} in $LaAlO_3$.

The level energies of the divalent and trivalent lanthanides in the bandgap of $GdAlO_3$ are well-established by optical spectroscopy, thermo-luminescence, and photo-conductivity studies [6, 18]. In this work a TL and spectroscopic study on $GdAlO_3$ doped with a trivalent lanthanide together with Cr^{3+} is presented. The level locations of Cr^{3+}, that may act as a hole trap to become Cr^{4+} and as an electron trap to become Cr^{2+}, within the bandgap and with respect to the vacuum level are derived.

We studied $GdAlO_3:Ce^{3+}$ together with Er^{3+}, Nd^{3+}, Ho^{3+}, Dy^{3+}, Tm^{3+}, and Sm^{3+} in [6]. Here Ce acts as deep hole trap and the co-dopant as shallow electron trap. The release of electrons during TL read-out resulting in Ce^{3+} UV emission occurs at temperature ranging from 150 K to 450 K that is consistent with the prediction from the VRBE scheme. For Sm^{3+} the glow peak maximum was predicted at temperatures where the Ce^{3+} emission is fully quenched and TL-glow is absent then. In this work we replace Ce^{3+} by Cr^{3+} that

appears also to act as a deep hole trap. By using the same co-dopants as in [6], the same glow peaks for electron release are observed. Since Ce^{3+} has been replaced by Cr^{3+}, the UV recombination emission is replaced by the infrared Cr^{3+} emission. This emission appears more temperature stable than the UV emission from Ce^{3+} which allows the detection of the Sm^{2+} glow peak. From a careful analyses of the TL-glow curves and the luminescence excitation spectra of Cr^{3+} emission, the Cr^{2+} and Cr^{3+} level locations in the band gap can be derived. It turns out that the Cr^{2+} ground state is in between the Sm^{2+} and Tm^{2+} ground states and the Cr^{3+} ground state is in between that of Ce^{3+} and Pr^{3+}. In addition to $GdAlO_3$ we also investigated Cr^{3+} in $LaAlO_3$. In $LaAlO_3$ the VRBE at the valence band is higher (less negative) and at the CB lower than in $GdAlO_3$. This causes that all TL peaks shift towards lower temperature and charge transfer bands towards lower energy.

II. EXPERIMENTAL METHODS

All starting materials were purchased from Sigma-Aldrich and used without further treatment. The appropriate stoichiometric mixture of Al_2O_3 (4N, 99.99%), rare earth oxides with a purity of 5N (99.999%) and Cr_2O_3 (4N, 99.99%) were weighted according to their chemical formula and milled homogeneously with the help of acetone. After drying, the powder was synthesized by heating at 1500 ^{o}C for 10 h in a corundum crucible with an atmosphere of N_2/H_2 (N_2:H_2 =93%:7%) to prevent oxidation of Cr to 4+. After that, the obtained compounds were cooled down to room temperature.

The photoluminescence excitation (PLE) and photoluminescence emission (PL) measurements were performed with a setup that consists of a UV/vis branch with a 500 W Hamamatsu CW Xe lamp and Gemini 180 monochromator and a VUV/UV branch using a deuterium lamp with an ARC VM502 vacuum monochromator. A Hamamatsu CCD camera was exploited as a detector connected at the exit slit of a Princeton Acton SP2300 monochromator. The sample is placed in an evacuated sample chamber and can be cooled down to 10K. Excitation spectra have been corrected for the lamp intensity at the monochromator exit slit.

TL measurements above room temperature (300 to 600 K) were performed with a Risø TL/OSL reader (model DA-15) and a controller (model DA-20). Samples were irradiated with a $^{90}Sr/^{90}Y$ β source with a dose rate of 0.7 mGy/s. Low temperature TL measurements

(90 to 450 K) were recorded with a sample chamber operating under vacuum ($P = 10^{-7}$ mbar), a $^{90}Sr/^{90}Y \beta$ irradiation source having a dose rate of ≈ 0.4 mGy/s, and a Perkin Elmer channel photomultiplier tube (MP-1393). Liquid nitrogen was used as a cooling medium. A filter to select the emission from Cr^{3+} was placed between the sample and the photomultiplier tube (PMT) during the measurements.

TL emission spectra (TLEM) were measured using a UV/vis spectrometer (Ocean Optics, QE65000) with a high-resolution composite grating (300 lines/mm) and an entrance aperture of 100 μm, resulting in a 3.3 nm (fwhm) wavelength resolution. The spectral range is 200 to 900 nm.

The TL excitation spectra (TLE) were measured by first illuminating the samples during 600 s with a monochromatic photon beam produced with a 150 W xenon arc lamp (Hamamatsu L2273) filtered by a 1/8 monochromator (Oriel Cornerstone 130) with wavelength resolution of 0.8 nm/0.1 mm slit width. The system is programmed to record all the TL glow curves from room temperature to 350 ^{o}C for the selected illumination wavelengths. The plot of the integrated TL glow peaks versus the illumination wavelength is called a TL excitation spectrum. A filter was placed between the sample and the PMT to monitor the glow from Cr^{3+}.

III. RESULTS

A series of GdAlO$_3$:Cr^{3+} samples co-doped with Nd^{3+}, Dy^{3+}, Tm^{3+}, and Sm^{3+} was synthesized and studied. Figure 1 shows the 10 K excitation spectrum of 740 nm Cr^{3+} emission in GdAlO$_3$ singly doped with Cr^{3+} in the UV/vis spectral region (spectrum a) and in the vacuum ultra violet (spectrum b). Besides the narrow Gd^{3+} 4f-4f excitation bands near 310 nm, 275 nm, and 250 nm, the transitions from the Cr^{3+} $^4A_2$ ground state to the $^4T_2(^4F)$ (562 nm), $^4T_1(^4F)$ (410nm), and the $^4T_1(^4P)$ (330 nm) excited states are observed. This all agrees with earlier work of de Vries et $al.$ [20] where the band (CT1) around 250 nm was attributed to a charge transfer band involving Cr^{3+}.

The excitation spectrum b) in the VUV region shows a second band CT2 near 195 nm. In the discussion we will assign band CT1 to electron transfer from Cr^{3+} to the conduction band, and band CT2 to electron transfer from the valence band to Cr^{3+}. The location of the host exciton creation band in GdAlO$_3$ has been identified near 170 nm (7.29 eV) in excitation
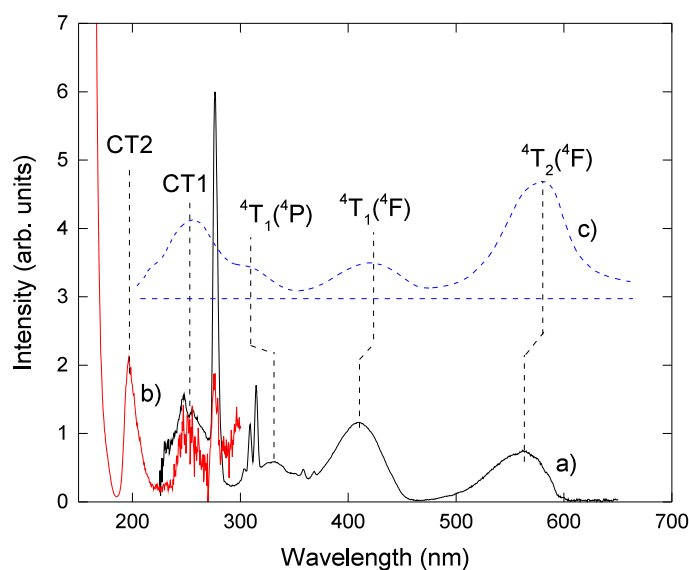
FIG. 1: a) UV/vis, and b) vacuum ultra violet excitation spectrum of 740 nm Cr^{3+} emission in $GdAlO_3$ at 10K. In c) the room temperature excitation spectrum of 734 nm Cr^{3+} emission in $LaAlO_3$ obtained from Katayama *et al.* [16] is shown.

spectra of Eu^{3+} [6], Ce^{3+} [21], and Tb^{3+} [19] luminescence. However, the exciton band is not observed in the excitation spectrum of Cr^{3+} emission, and apparently the energy transfer from a bound electron-hole pair to Cr^{3+} is inefficient. At shorter than 160 nm, energy is sufficient to create free electrons and free holes, and efficient transfer does occur.

Figure 2b) and d) show the low temperature thermoluminescence spectra of $GdAlO_3:Ce^{3+}$ co-doped with Nd^{3+} and Dy^{3+}. The glow peaks at 165 K and at 245 K were attributed in [6] to the release of an electron from Nd^{2+} and Dy^{2+} that recombines with Ce^{4+} yielding Ce^{3+} 5d-4f emission. The same glow peaks are also observed when Ce^{3+} is replaced by Cr^{3+} in Fig. 2a) and c). Both glow peaks are absent in single Cr^{3+} doped $GdAlO_3$ in Fig. 2e).

Figure 3 shows TL glow curves for Cr^{3+} only and when Tm^{3+} and Sm^{3+} are the co-dopants. The glow peak around 475 K with a glow tail extending down to 325K is common to all three spectra. Tm^{3+} gives a weak additional glow around 410K which is at the same temperature as in $GdAlO_3:Ce^{3+},Tm^{3+}$ in [6] where it was attributed to electron release from Tm^{2+}. Sm^{3+} co-doping gives a clear glow peak with maximum around 525K. In addition, a weak glow is observed around 600 K for all three spectra.
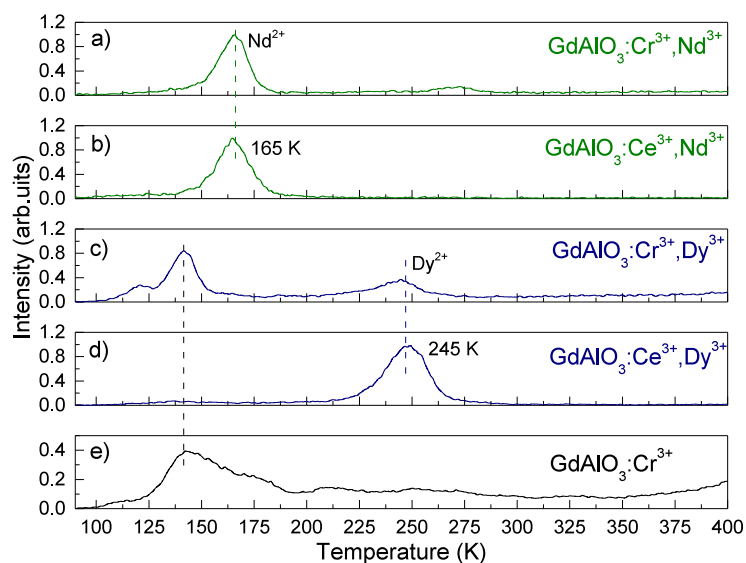
FIG. 2: Low temperature TL spectra of Cr^{3+} and Ln^{3+} doped $GdAlO_3$ samples. The infrared emission of Cr^{3+} was monitored in spectra a), c) and e), and the UV emission of Ce^{3+} in spectra b) and d). A heating rate of 1 K/s was used.
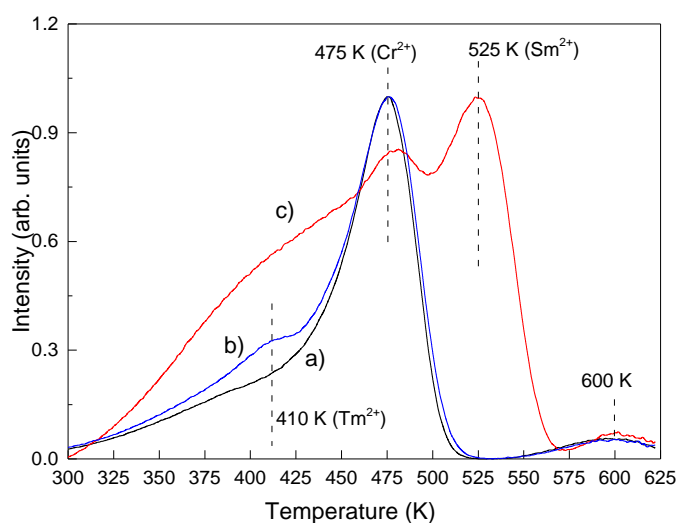

FIG. 3: Thermoluminescence glow curves after β-irradiation of a) non co-doped $GdAlO_3:Cr^{3+}$, b) with Tm^{3+} co-doping, and c) with Sm^{3+} co-doping at a heating rate of 1 K/s. The infrared emission of Cr^{3+} was monitored.

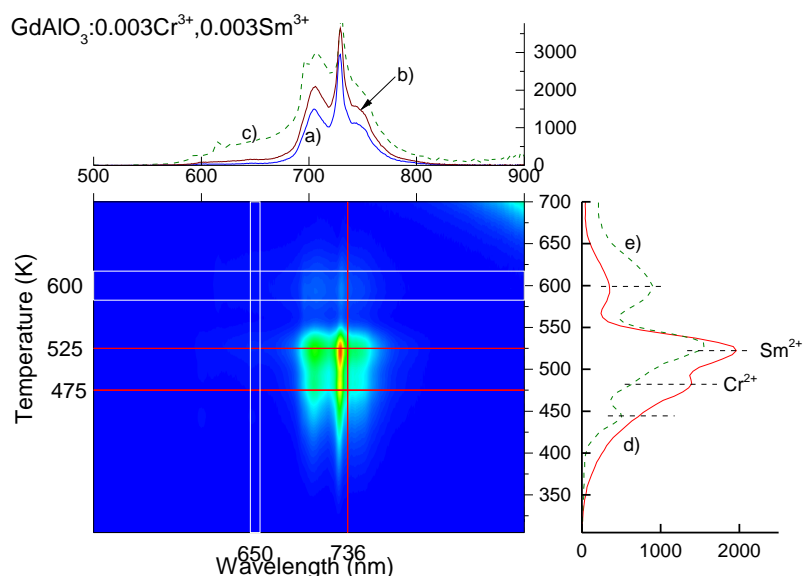Figure 4 shows the thermoluminescence emission spectrum of $GdAlO_3:Cr^{3+},Sm^{3+}$. The

FIG. 4: Thermoluminescence emission spectra of $GdAlO_3$:Cr^{3+},Sm^{3+} at a heating rate of 1 K/s. The emission glow at a temperature of 475 K and 525 K is projected on top as spectrum a) and b). The integrated glow between 590 K and 610 K is in spectrum c). The TL at 736 nm emission is projected on the right side as spectrum d), and the TL of the integrated emission between 646 nm and 654 nm as spectrum e). The projection points and intervals are indicated by the horizontal and vertical lines.

projection at the main Cr^{3+} emission around 736 nm (spectrum d) shows a TL-curve similar to that in Fig. 3c). The projected luminescence at a glow temperature of 475 K (spectrum a) is almost entirely from Cr^{3+} emission. The emission at 525 K (spectrum b) is mainly from Cr^{3+} together with a weak broad luminescence that starts at 600 nm and seems to extend towards 675 nm. The glow around 600 K (spectrum c) reveals both Cr^{3+} and broad band emission. If a TL projection is made at the weak broad band emission around 650 nm spectrum e) appears.

We verified that in the TL-emission spectrum of $GdAlO_3$ singly doped with Cr^{3+} the same TL spectrum as in Fig. 3a) appears. The glow below 440 K is exclusively from Cr^{3+}. A projection made at 475 K (not shown), reveals that 95% of the luminescence is from Cr^{3+}, and the rest is broad band 600-675 nm emission. A projection made at 600 K (not shown) reveals that both emissions are present of about similar integral intensity. This is, apart from the glow peak at 525 K, all quite similar as observed in Fig. 4.
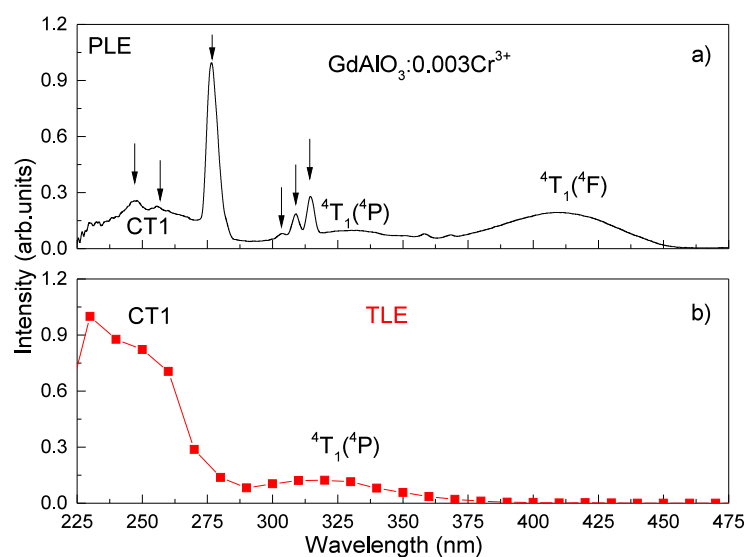
FIG. 5: a) The photoluminescence excitation spectrum of Cr^{3+} emission in $GdAlO_3$, and b) the thermoluminescence excitation spectrum of $GdAlO_3:Cr^{3+},Sm^{3+}$.

Figure 5 compares the photoluminescence excitation spectrum from Fig. 1a) with the thermoluminescence excitation spectrum of $GdAlO_3:Cr^{3+}$. The results show that the phosphor can be charged when Cr^{3+} is excited to the $^4T_1(^4P)$ excited state but it does not charge when excited to lower energy states. Excitation in the CT1 band near 250 nm gives very strong charging. Gd^{3+} excitation lines (see the down pointing arrows in spectrum a) are not observed in the TLE spectrum. Although the Gd peaks will appear less sharp due to the limited 8 nm resolution in the TLE spectrum, it seems that excitation of Gd does not lead to efficient charging of the phosphor.

Figure 6 shows the thermoluminescence emission spectrum of $LaAlO_3:Cr^{3+}$ and Fig. 7 when also Sm^{3+} co-dopants are present. The Cr^{3+} only sample shows a TL-glow peak near 379 K (spectrum c) that generates Cr^{3+} emission only (spectrum a). There is also an intense glow near 509 K that generates Cr^{3+} emission between 700 and 800 nm but also a weak broad emission band between 600 and 675 nm (spectrum b). The TL spectrum at the broad band emission (spectrum d) shows the slightly shifted 509 K TL peak (spectrum d). Fig. 7c) shows that with Sm^{3+} co-doping, a new TL-peak appears at 360 K where the glow is entirely from Cr^{3+} as shown in spectrum a). Again the 509 K glow is observed that generates besides glow from Cr^{3+} also glow from the broad band emission between 600 and
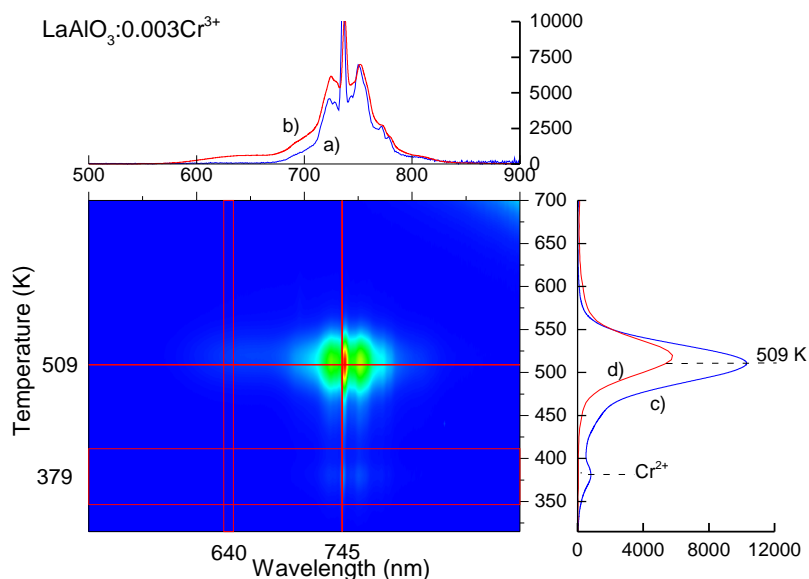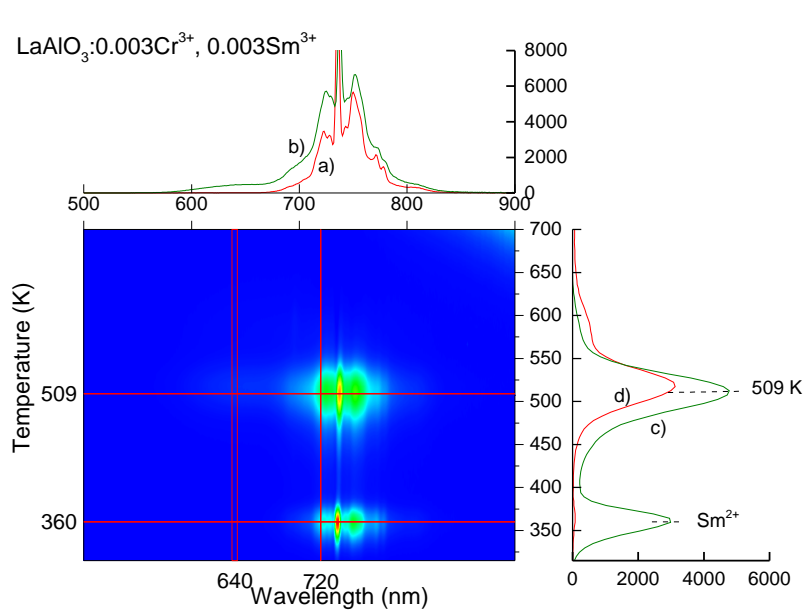
FIG. 6: TL emission spectra of LaAlO$_3$ singly doped with Cr^{3+} at a heating rate of 1 K/s. The integrated emission glow between 372 K and 386 K is projected on top as spectrum a). The emission glow at 509 K is projected as spectrum b). The emission at 735 nm is projected on the right side as TL spectrum c). The integrated emission between 635 nm and 645 nm is projected as TL-spectrum d). The projection points and intervals are indicated by the horizontal and vertical lines.

675 nm as seen in spectrum b).

IV.   DISCUSSION

In an earlier work we studied the TL properties of GdAlO$_3$ doped with various combinations of two lanthanides, one acting as hole trapping center and the other as electron trapping center [6]. Figure 8 shows the VRBE diagram for the lanthanides in GdAlO$_3$ as derived in that work. For Ce^{3+} combined with Er^{3+}, Nd^{3+}, Ho^{3+}, Dy^{3+}, and Tm^{3+} we identified glow peaks associated with the release of an electron that recombines with the hole trapped on Ce. The temperatures T_m at the maximum of the glow peaks are indicated at the top of the VRBE scheme. The T_m for electron release from Sm^{2+} was predicted at 587 K in [6]. It could not be observed in GdAlO$_3$:Ce^{3+},Sm^{3+} because of strong thermal quenching of Ce^{3+} emission. Fig. 2a) and c) demonstrate that when Ce^{3+} is replaced with

FIG. 7: The TL emission spectra of $LaAlO_3:Cr^{3+}$ codoped with Sm^{3+} at a heating rate of 1 K/s. At the top, the emission at the glow temperature of 360 K and 509 K is projected as spectrum a) and b), respectively. The TL-spectrum at the Cr^{3+} emission of 720 nm is projected at the right as spectrum c), and the TL-spectrum of the integrated luminescence intensity between 637 nm and 643 nm is projected as spectrum d). The projection points and intervals are indicated by the horizontal and vertical lines.

Cr^{3+} the TL-glow curves appear at the same temperature. Evidently electrons are released from the divalent lanthanides and recombine at Cr^{4+}.

Figure 9 shows T_m against the trap depth $E_t = E_C - E(Ln^{2+})$ where E_C is the VRBE at the bottom of the CB and $E(Ln^{2+})$ in the ground state of Ln^{2+}. To good approximation a proportional relationship is to be expected. A linear fit through the data without Sm^{2+} gives a slope of 315 K/eV and an intercept at -0.1 eV. The intercept close to zero indicates that the VRBE diagram agrees very well with observed trapping depths. From the linear fit $T_m(Sm^{2+})$ is expected near 560K. For the Sm^{3+} co-dopant a new TL-glow peak appears in Fig. 3c) at 525K. Although at 35 K lower temperature than predicted, we still attribute it to the release of an electron from Sm^{2+} that then recombines with Cr^{4+} to yield Cr^{3+} emission. We allow for a deviation because the band gap and related energy E_C always tend to lower when temperature increases. This means that the electron trap depths decrease with increase of temperature. The effect is then strongest for the high temperature glow
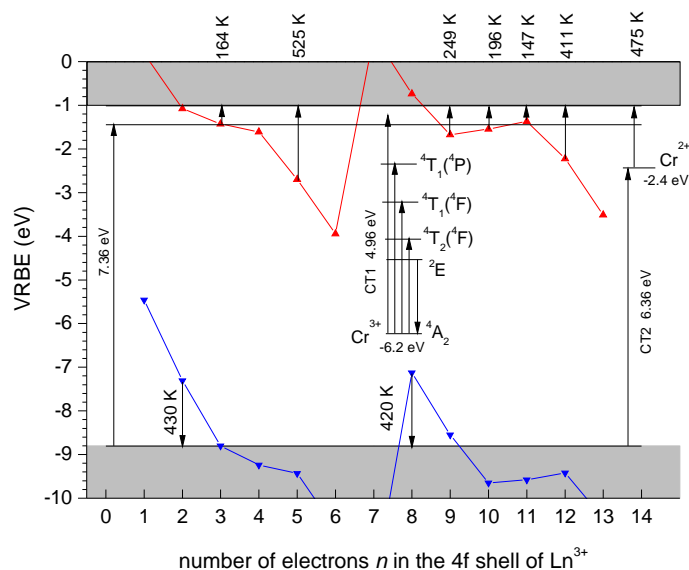
FIG. 8: The VRBE diagram for the lanthanides and chromium in $GdAlO_3$. The different electron and hole transfer processes with energies identified with thermoluminescence and spectroscopy are indicated. The temperature T_m of the TL glow peak maximum found at a heating rate of 1 K/s for the release of an electron from divalent Nd, Sm, Dy, Ho, Er, Tm, Cr and tetravalent Pr and Tb are indicated.

peak of Sm^{2+}. For the lanthanides in $LaPO_4$ one may observe a similar phenomenon [4].

Since the electron is released from Sm^{2+} to recombine with Cr^{4+}, the hole on Cr^{4+} must be more strongly trapped than the electron on Sm^{2+}. The glow peak at 475K, in between that of Tm^{2+} and Sm^{2+}, is common to all three TL-spectra of Fig. 3, and its emission is from Cr^{3+}. Either an electron is released that recombines with Cr^{4+} or a hole is released to recombine with Cr^{2+}. This latter option can be ruled out because such hole would also recombine with Sm^{2+} to generate Sm^{3+} emission which is not observed. Apparently there is an electron trap with ground state in between the ground states of Tm^{2+} and Sm^{2+}. The 600 K glow peak observed in Fig. 3 and in Fig. 4 is attributed to an unknown deep electron trap. The released electron recombines with Cr^{4+} to yield Cr^{3+} emission. It can also recombine with an unknown deep hole trap to yield the broad band 600 to 675 nm emission. Apparently the release of a hole from Cr^{4+} does not occur before 600K. We know from [6] that the hole on Pr^{4+} and Tb^{4+} in $GdAlO_3$ is released at 430 K and 420 K, and this implies that the Cr^{3+} ground state must be at least 0.5 eV above that of Pr^{3+} and Tb^{3+} in
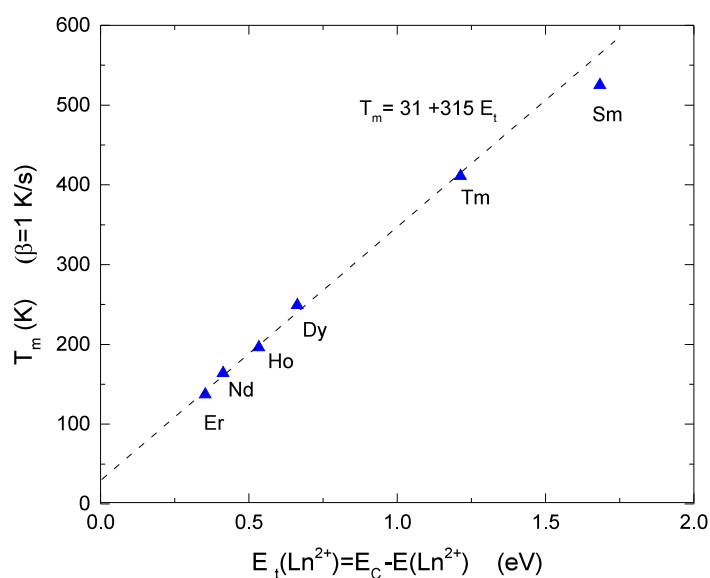
FIG. 9: The temperature T_m of the glow peak maximum due to electron release from divalent lanthanides recorded at a heating rate of 1 K/s as a function of the trap depth derived from the VRBE scheme.

the band gap of $GdAlO_3$.

Cr^{3+} as an electron trapping center has been studied extensively in the $Y_3(Al_{1-x}Ga_x)_5O_{12}$ garnet compounds. It was found that the VRBE in the Cr^{2+} ground state is -2.75 eV $\pm$ 0.06 eV for all compositions [14, 15]. From Rogers et $al.$ [22] we know that the VRBE in the lowest Ce^{3+} 5d-state or lowest Ti^{3+} 3d state show a compound to compound variation of usually less than $\pm$ 0.7 eV. For the VRBE in the $3d^3$ transition metal Cr^{3+} we also do not expect large compound to compound variation. According to Fig. 9, a 475K glow peak corresponds with 1.4 eV trap depth which translates to -2.4 eV in the VRBE scheme. This would be consistent with the about to expect location of the Cr^{2+} ground state, and we therefore assign the 475 K glow to the release of an electron from Cr^{2+} as indicated in Fig. 8.

The excitation spectra of Cr^{3+} in the UV/vis and in the VUV in Fig. 1 show a band near 250 nm (CT1) and 195 nm (CT2). With a location of the Cr^{2+} ground state near -2.4 eV, the VB→Cr^{3+} electron transfer band is expected at 6.4 eV. The CT2 band at 195 nm (6.36 eV) corresponds perfectly with this energy, and we therefore assign the CT2 band to such

Journal of Materials Chemistry C Accepted Manuscript

electron transfer. The CT1 band at 250 nm (4.96 eV) is now attributed to the Cr^{3+}-CB electron transfer. It would translate to a VRBE of -6.2 ± 0.2 eV for the Cr^{3+} ground state energy in agreement with a location of at least 0.5 eV above that of Pr^{3+} at -7.3 eV and Tb^{3+} at -7.1 eV.

With the proposed locations of the Cr^{2+} and Cr^{3+} ground states we can interpret the TL excitation spectrum of Fig. 5. Excitation in the CT1 band excites electrons from Cr^{3+} to the conduction band that are trapped by another Cr^{3+} to form Cr^{2+} or by the deep electron trap responsible for the 600 K glow peak. Excitation in the Cr^{3+} $^4T_1(^4P)$ excited state also leads to trap filling. Fig. 8 shows that the VRBE in the $^4T_1(^4P)$ level is near -2.3 eV which is still well below the CB-bottom, and charging via the CB seems improbable at RT. However, because the $^4T_1(^4P)$ level is above the Cr^{2+} ground state energy, an electron transfer in close pair Cr^{3+} centers is energetically possible after the $^4T_1(^4P)$ level is populated. There are experimental indications that the reversed electron transfer from Cr^{2+} to Cr^{4+} also takes place. All TL-spectra in Fig. 3 and Fig. 4 show, starting at RT, increasing athermal glow intensity up to 450K. Above 450K, the 475 K glow peak from Cr^{2+} electron release appears. Similar athermal glow was observed and studied in the YPO_4 system with various combinations of lanthanide dopants, and attributed to a tunneling type of recombination [23]. In our case, the electron transfers from the Cr^{2+} ground state to a nearby Cr^{4+} center to enter into an excited Cr^{3+} level at lower VRBE followed by the infrared Cr^{3+} emission. Such mechanism is fully consistent with the Cr^{3+} and Cr^{2+} ground and excited state level locations in the VRBE scheme.

Now that we have arrived at a fully consistent interpretation of the spectroscopic and TL data with the VRBE level locations of all dopants involved, one may compare the results for $GdAlO_3$ with result for $LaAlO_3$. Large differences in the VRBE energies of the lanthanides or Cr dopants between the two compounds are not to be expected, and the largest effect is from a different energy at the CB-bottom and VB-top. This has direct consequence for the energy of CT-bands and electron and hole trap depths.

The VRBE scheme for $LaAlO_3$ has been presented at various occasions but with different values for the host exciton energy E^{ex} and the band gap. The uncertainty is due to lack of experimental data in the vacuum ultra violet. In Luo et $al.$ [6] we presented the vacuum ultra violet excitation spectrum of Eu^{3+} emission that showed a very broad host excitation band starting already at 215 nm (5.77 eV) and extending to 155 nm (8.0 eV). For E^{ex} we
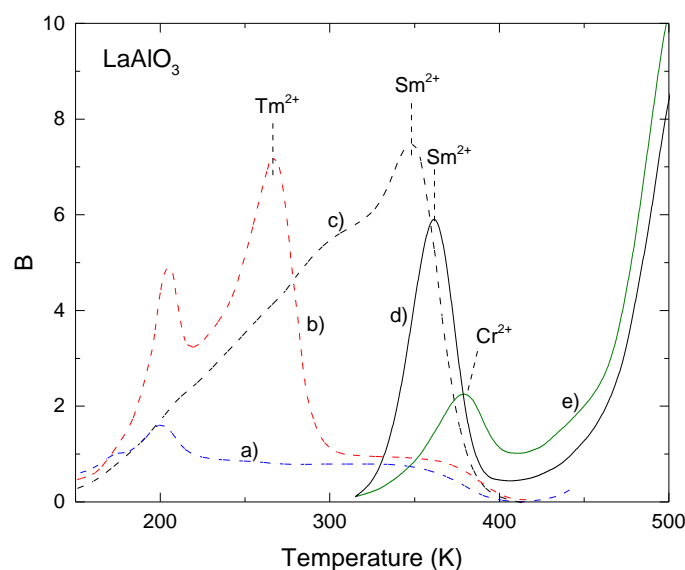
FIG. 10: TL spectra for Cr^{3+} doped and Sm and Tm co-doped $LaAlO_3$. Spectra a) for single Cr^{3+} doped, b) for Tm^{3+} co-doped, and c) for Sm^{3+} co-doped $LaAlO_3$ are redrawn from Katayama *et al.* [17] and were recorded at a heating rate of 10 K/min. Spectra d) for Sm co-doping and e) for single Cr doping are from this work recorded at 1 K/s.

used a value of 6.36 eV but in Ref. [24] a value of 5.9 eV was used. Below we will use TL-data to locate the conduction band bottom.

The results in this work for $GdAlO_3$:Cr^{3+},Ln^{3+}, in many respects, resemble those for $LaAlO_3$:Cr^{3+},Ln^{3+} as studied by Katayama *et al* [16, 17]. TL-spectra for $LaAlO_3$ singly doped and co-doped with Tm^{3+} and Sm^{3+} from those works are redrawn in Fig. 10. Using a heating rate of 10K/min, they observed TL glow peaks at 350K (see spectrum c) and 270K (see spectrum b) that were attributed to electron release from Sm^{2+} and Tm^{2+}, respectively. Our result for Sm and Cr doped $LaAlO_3$ in Fig. 7c) is shown as spectrum d) in Fig. 10. The observed glow peak at 360 K must, following Katayama *et al.*, now be attributed to the release of an electron from Sm^{2+} that recombines with Cr^{4+}. The 10 K higher temperature is due to the higher heating rate of 1 K/s in our studies.

Katayama *et al.* noticed a strong athermal Cr^{3+} glow starting at 150 K up to 380-390 K present for the Cr only sample, see spectrum a) in Fig. 10. It appears even stronger when the co-dopants Sm or Tm are present. The athermal glow in $LaAlO_3$ drops down to
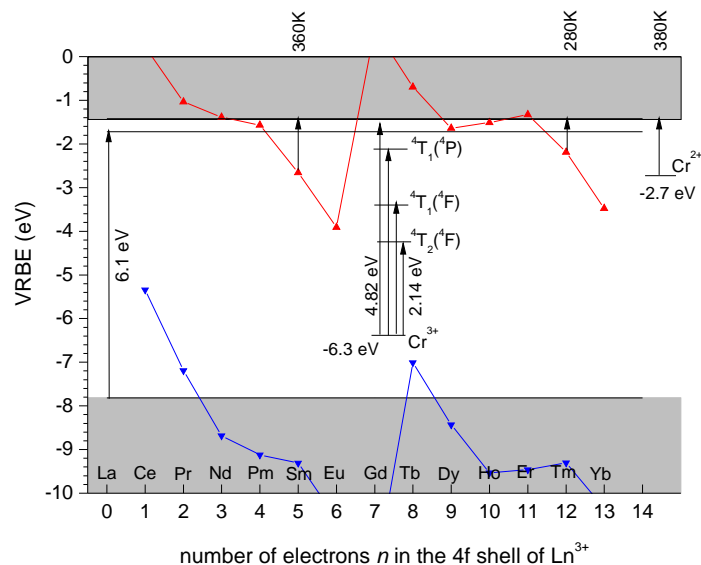
FIG. 11: The VRBE diagram for the lanthanides and chromium in $LaAlO_3$ constructed with E^{ex}=6.05 eV, U=6.67 eV and $E^{CT}(Eu)$=3.91 eV. The temperature T_m of the TL glow peak maximum found at a heating rate of 1 K/s for the release of an electron from divalent Sm, Tm, Cr are indicated.

a lower level the moment the Tm^{2+} (spectrum b) or Sm^{2+} (spectrum c) glow peak appears. This evidences that the electron transfers directly from the ground state of Tm^{2+} or Sm^{2+} to a nearby Cr^{4+} to enter an excited state of Cr^{3+}. In the Cr only sample the athermal glow persists until 380 K, and this is precisely where we observe the 379 K glow peak (see spectrum e) in our sample. The 379K glow peak is therefore attributed to electron release from Cr^{2+} to the CB, and the athermal glow between 150 and 380K in the work of Katayama *et al.* is then from the tunneling recombination between Cr^{2+} and Cr^{4+}.

Figure 11 shows the VRBE scheme of $LaAlO_3$ constructed with a U-parameter U=6.67 eV and 3.91 eV for the energy of the Eu^{3+} CT-band. The T_m for the Tm^{2+} and Sm^{2+} glow peaks in $LaAlO_3$ are 130K to 165K lower than in $GdAlO_3$. Using the 315 K/eV dependence from Fig. 9, we estimate 0.4-0.5 eV less deep electron traps in $LaAlO_3$. Apparently, the CB-bottom in $LaAlO_3$ is at 0.4-0.5 eV lower VRBE than in $GdAlO_3$. To arrive at such situation E^{ex} for $LaAlO_3$ must be about 6.1 eV, and this was used in the scheme for $LaAlO_3$. Now one can also locate the Cr^{3+} and Cr^{2+} ground state levels. The 380 K glow peak from Cr^{2+} translates to a ground state energy 0.06 eV below that of Sm^{2+} bringing it near -2.7 eV in

Fig. 11. Note that for the $Y_3(Al_{1-x}Ga_x)_5O_{12}$ garnet family of compounds the Cr^{2+} ground state was found at -2.75 eV which is quite the same.

To locate the ground state of Cr^{3+} we can use the excitation spectrum of Cr^{3+} emission presented by Katayama *et al.* [16, 17] and redrawn in Fig. 1 spectrum c). It is similar to the one for $GdAlO_3$ with slightly shifted excitation bands. Other than in Katayama *et al.*, we attribute the 257 nm band (4.82 eV) to the $Cr^{3+}{\rightarrow}CB$ electron transfer and the weaker band at 305 nm to the $^4T_1(^4P)$ band. Using the 4.82 eV CT band energy the Cr^{3+} ground state is found near -6.3±0.2 eV in Fig. 11.

Comparing the Cr^{3+} and Cr^{2+} location in $GdAlO_3$ with that in $LaAlO_3$, the VRBEs in $LaAlO_3$ appears at few 0.1 eV lower energy. This is not really significant because the errors in VRBE energies are of the same magnitude. In any case we conclude that the VRBE in the ground state of Cr^{2+} and Cr^{3+} for $GdAlO_3$ and $LaAlO_3$ are quite similar, and expectedly the same will apply for $YAlO_3$ and $LuAlO_3$. Since the Cr^{2+} location is also at similar energy in the $Y_3(Al_{1-x}Ga_x)_5O_{12}$ garnet family, our findings suggests that the values found for Cr^{2+} and Cr^{3+} VRBE energies may hold quite generally when Cr^{3+} is on an octahedral oxygen coordinated Al or Ga-site.

V.   SUMMARY AND CONCLUSIONS

We have obtained a consistent interpretation of the TL- and photoluminescence excitation spectra of Cr^{3+} doped and Ln^{3+} co-doped $GdAlO_3$ and $LaAlO_3$. The Cr^{2+} ground state in $GdAlO_3$ is found near -2.4 to -2.5 eV in $GdAlO_3$ that is in between that of Sm^{2+} and Tm^{2+}. The location is few 0.1 eV lower in $LaAlO_3$ bringing it slightly below that of Sm^{2+}. Cr^{3+} acts therefore as an electron trapping center in those two compounds. The Cr^{3+} ground state is found near -6.2 eV and -6.4 eV which is in between that of Ce^{3+} and Pr^{3+}. It means that Cr^{3+} can act not only as an electron trapping center but also as a deep hole trapping center. This is different from all the lanthanides that either act as electron trap or as hole trap. We have identified an athermal recombination luminescence in $GdAlO_3$. The electron trapped in Sm^{2+}, Tm^{2+}, or Cr^{2+} can transfer to a nearby Cr^{4+} center to populate an excited state of Cr^{3+} to generate Cr^{3+} emission. This is possible because the Sm^{2+} and Tm^{2+} ground state levels are above the excited Cr^{3+} level in the VRBE diagram. The situation in $LaAlO_3$ appears very similar but because of an about 0.5 eV lower lying conduction band bottom,

TL glow peaks appear at lower temperature.

[1] P. Dorenbos, Phys. Rev. B 85 (2012) 165107.

[2] A.J.J. Bos, P. Dorenbos, A. Bessiere, B. Viana, Radiation Measurements 43 (2008) 222.

[3] Y. Katayama, T. Kayumi, J. Ueda, P. Dorenbos, B. Viana, S. Tanabe, J. Mater. Chem. C, 5 (2017) 8893.

[4] Tianshuai Lyu, Pieter Dorenbos, J. Mat. Chem. C. 6 (2018) 369.

[5] E.D. Millikin, L.C. Oliveira, G. Denis, E.G. Yukihara, J. Lumin. 132 (2012) 2495.

[6] Hongde Luo, Adrie J. J. Bos, and Pieter Dorenbos, J. Phys. Chem. C 120 (2016) 5916

[7] Yixi Zhuang, Ying Lv, Ye Li, Tianliang Zhou, Jian Xu, Jumpei Ueda, Setsuhisa Tanabe, Rong-Jun Xie, Inorg. Chem. 55 (2016) 11890

[8] Y. Miyamoto, H. Kato, Y. Honna, H. Yamamoto, K. Ohmi, J. Elechtrochem. Soc. 156 (2009) J235.

[9] A. Bessiere, S. Jacquart, K. Priolkar, A. Lecointre, B. Viana, D. Gourier, Optics Express 19 (2011) 10131.

[10] Zhengwei Pan, Yi-Ying Lu, Feng Lu, Nature Materials. 11(1) (2012) 58.

[11] Yixi Zhuang, Jumpei Ueda, Setsuhisa Tanabe and Pieter Dorenbos, J. Mater. Chem C, 2 (2014) 5502.

[12] T. Maldiney, A. Bessiere, J. Seguin, E. Teston, S.K. Sharma, B. Viana, A.J.J. Bos, P. Dorenbos, M. Bessodes, D. Gourier, D. Scherman, C. Richard, Nature Materials 13 (2014) 418.

[13] Jinlei Li, Chengcheng Wang, Junpeng Shi, Penghui Li, Zhenfeng Yu, Hongwu Zhang, Journal of Luminescence 199 (2018) 363.

[14] J. Ueda, K. Kuroishi, S. Tanabe, Appl. Phys. Lett. 104 (2014) 101904.

[15] J. Ueda, P. Dorenbos, A. J. J. Bos, K. Kuroishi, S. Tanabe, J. Mater. Chem. C 3 (2015) 5642.

[16] Y. Katayama, H. Kobayashi, S. Tanabe, Appl. Phys. Express 8 (2015) 012102.

[17] Yumiko Katayama, Hiroaki Kobayashi, Jumpei Ueda, Bruno Viana, Setsuhisa Tanabe, Opt. Mater. Express 6 (2016) 257134.

[18] P. Dorenbos, Opt. Materials 69 (2017) 8.

[19] Yuhua Wang, Hui Gao, Electrochem. and Solid State Lett. 9 (2006) H19.

[20] A.J.de Vries, W.J.J. Smeets, G. Blasse, Materials Chemistry and Physics, 18 (1987) 81.

Journal of Materials Chemistry C Accepted Manuscript

[21] J.W.M. Verweij, M.Th. Cohen-Adad, D. Bouttet, H. Lautesse, C. Pedrini, Chem. Phys. Lett. 239 (1995) 51.

[22] E.G. Rogers. P. Dorenbos, J. Lumin. 153 (2014) 40.

[23] A. Dobrowolska, A.J.J. Bos, P. Dorenbos, J. Phys. D: Appl. Phys., 47 (2014) 335301.

[24] P. Dorenbos, Phys. Rev. B 87 (2013) 035118.

Journal of Materials Chemistry C Accepted Manuscript

18